# Nitrogen-15 NMR Study of Solid Cobaloximes Containing $^{15}$N-Labeled Pyridine and Aniline

**Robert W. Schurko and Roderick E. Wasylishen***

*Department of Chemistry, Dalhousie University, Halifax, Nova Scotia, Canada B3H 4J3*

*Received: December 3, 1999; In Final Form: January 20, 2000*

Solid-state $^{15}$N NMR spectra of spinning and stationary samples of four cobaloximes containing either pyridine-$^{15}$N or aniline-$^{15}$N as ligands are presented. The cobaloximes investigated are py$Co(DH)_2Cl$ (**1**), py$Co(DH)_2Br$ (**2**), py$Co(DH)_2CH_3$ (**3**), and anil$Co(DH)_2Cl$ (**4**) where DH = the dimethylglyoxime anion, py = pyridine, and anil = aniline. Nitrogen-15 CPMAS NMR spectra exhibit $^{15}$N, $^{59}$Co residual dipolar coupling, due to the breakdown of the high-field approximation for the $^{59}$Co ($S = 7/2$) nuclei. These spectra are analyzed to yield the one-bond cobalt-nitrogen indirect spin−spin coupling constant, $^1J(^{59}Co,^{15}N)$, as well as the magnitude and sign of the $^{59}$Co nuclear quadrupole coupling constant, $C_Q$, and the orientation of the electric field gradient tensor at the $^{59}$Co nucleus with respect to the molecular frame. Nitrogen-15 NMR spectra of stationary samples are analyzed using the dipolar-chemical shift method, providing the principal components of the nitrogen chemical shift tensors and information concerning their orientations with respect to the molecular frame. The sign of $^1J(^{59}Co,^{15}N)$ is also determined from these spectra. The ab initio gauge-independent atomic orbital (GIAO) method is used to calculate the nitrogen chemical shielding tensors for three of the cobaloximes, as well as for free pyridine and aniline. Comparison of experimental and theoretical data reveals qualitative agreement, and supports the experimentally proposed nitrogen chemical shielding tensor orientations. The nitrogen coordination shifts and chemical shielding tensor orientations of pyridine- and aniline-substituted cobaloximes can qualitatively be accounted for using molecular orbital theory.

## Introduction

Cobaloximes are a class of compounds containing the $Co^{(III)}(DH)_2^+$ moiety, where DH is a monoanion of dimethylglyoxime (Figure 1). The nitrogen atoms of the glyoxime moiety are situated in an approximately rectangular planar arrangement about the central cobalt atom. Typical cobaloximes have one neutral ligand (L) and one anionic ligand (X) in the axial positions, and a pseudo-octahedral arrangement about the central cobalt atom. Most cobaloximes possess an approximate $C_2$ axis and have near-$C_{2v}$ symmetry. Cobaloximes have been of great interest to chemists for the past 40 years for two major reasons. First, the coordination chemistry of these complexes is far-reaching, with almost unlimited possibilities for substituents in the axial positions and variations on the nature of the equatorial ligands.[1] Second, there are many organometallic cobaloxime derivatives which have been used as model compounds for the study of biologically important systems, such as vitamin $B_{12}$.[2] Though there have been a large number of solution NMR studies on the cobaloximes[3] and related compounds,[4] only four solid-state NMR studies on the cobaloximes have been reported in the literature.[5−7] LaRossa and Brown reported the results of a comprehensive $^{59}$Co (spin 7/2) NQR investigation of cobaloximes.[8] Values of the $^{59}$Co nuclear quadrupole coupling constant, $C_Q$, and the asymmetry parameter, $\eta$, were reported; however, the orientation of the electric field gradient (EFG) tensor at the cobalt nucleus could only be predicted in a qualitative manner. It is also noted that a solid-state $^{59}$Co NMR study has been conducted on a single crystal of vitamin $B_{12}$, in which the orientations of the electric field gradient tensor and chemical shift tensor have been determined unambiguously.[9]

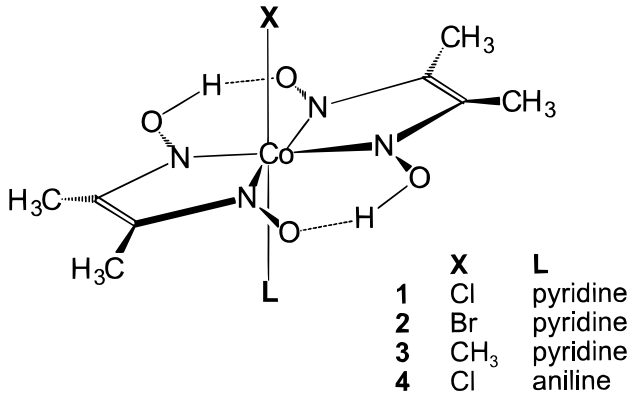


| | X | L |
|---|---|---|
| **1** | Cl | pyridine |
| **2** | Br | pyridine |
| **3** | $CH_3$ | pyridine |
| **4** | Cl | aniline |

**Figure 1.** The molecular structure of cobaloximes, with anionic species (X) and neutral ligands (L) substituted into the axial positions.

The purpose of this paper is to demonstrate the wealth of information that is available from solid-state $^{15}$N NMR studies on cobaloximes, $LCo(DH)_2X$, in which L = $^{15}$N-enriched pyridine or aniline, and X = $Cl^-$, $CH_3^-$, and $Br^-$. Nitrogen-15 magic-angle spinning (MAS) NMR spectra obtained under conditions of cross-polarization (CP) provide much information not available from solution NMR studies. Specifically, the first values of $^1J(^{59}Co,^{15}N)$ in cobaloximes are reported. Furthermore, it is demonstrated that information regarding the orientation of the $^{59}$Co EFG tensor can be extracted indirectly by examining the $^{15}$N CPMAS NMR spectra, due to the presence of residual dipolar coupling between the $^{15}$N and $^{59}$Co nuclei.[10−12] To the best of our knowledge, there are only three other reports of $^1J(^{59}Co,^{15}N)$, all of which were obtained from solution $^{15}$N NMR studies.[13,14] The only other *J*-couplings available for comparison are $^1J(^{103}Rh,^{15}N)$ values reported for the rhodium analogues of

* Author to whom correspondence should be addressed. Phone: 902-494-2564. Fax: 902-494-1310. E-mail: rodw@is.dal.ca.

10.1021/jp994254m CCC: $19.00 
Published on Web 03/28/2000

cobaloximes, the rhodoximes,[15] and other six-coordinate rhodium complexes.[16]

In addition, nitrogen chemical shielding (CS) tensors of the pyridine and aniline ligands are characterized via analysis of the $^{15}$N NMR spectra of stationary samples using the dipolar-chemical shift method.[17] Results are compared with those recently reported for the free pyridine-$^{15}$N ligand.[18] A large number of nitrogen CS tensors in a variety of organic and inorganic complexes have been reported in the literature.[19,20] More specifically, there have been several accounts of nitrogen CS tensors of nuclei directly coordinated to transition metals.[21−24] Recent reports include nitrogen CS tensors in tetraphenylporphyrin complexes by Grant and co-workers,[25] and in nitrosoarene−metal complexes[26] and metalloporphyrins[27] by Oldfield et al. Ab initio calculations of nitrogen shielding tensors have also been conducted on such systems by Oldfield and co-workers,[26,27] as well as de Dios et al.[28] Though nitrogen CS tensor orientations are available from ab initio calculations, we are aware of only one transition-metal compound where the nitrogen chemical shift tensor has been inferred from experiment.[24]

Finally, modern first-principles calculations of nitrogen CS tensors in pyridine- and aniline-substituted cobaloximes are presented, along with calculations on the uncoordinated ligands. The ab initio calculations provide insight into the experimentally determined nitrogen CS tensor principal components, as well as the orientation of the CS tensor with respect to the molecular frame.

## Experimental Section

Nitrogen-15-labeled (99%) py$Co(DH)_2Cl$ (**1**) and anil$Co(DH)_2Cl$ (**4**) were synthesized from $Co(DH)(DH_2)Cl_2$[29] and $^{15}$N-labeled pyridine and aniline according to standard literature methods.[3a,30] Pyridine-$^{15}$N and aniline-$^{15}$N (99%) were obtained from Cambridge Isotope Laboratories and used without further purification. Samples of $^{15}$N-py$Co(DH)_2Br$ (**2**) and $^{15}$N-py$Co(DH)_2CH_3$ (**3**) ($^{15}$N-labeling, ca. 25%) were synthesized from $Co(DH)(DH_2)Br$ and pyridine-$^{15}$N using an adaptation of a recently published synthetic method.[31] Due to the small amounts of starting material for complexes **2** and **3** (ca. 30−50 mg), the $^{15}$N-labeled compounds were mixed with freshly prepared, natural abundance samples in order to provide enough material to fill the NMR rotors. Crystalline samples were powdered and packed into 7 mm o.d. and 4 mm o.d. zirconium oxide rotors.

Solid-state $^{15}$N CP NMR spectra of both spinning (MAS) and stationary samples were acquired at 20.3 MHz (4.7 T) and 40.5 MHz (9.4 T) on Bruker MSL-200 and AMX-400 NMR spectrometers. Typical spinning rates for the 7 mm o.d. rotors were between 2.0 and 3.5 kHz; for the 4 mm rotors, spinning rates ranged from 5.0 to 10.5 kHz. Contact times were between 5 and 10 ms, and 90° pulses of 6.0 to 6.5 $\mu$s were applied. All spectra were acquired with high-power proton decoupling. Nitrogen-15 CPMAS NMR spectra were acquired with ca. 2000−8000 scans, while spectra of stationary samples were acquired with 13000−22000 scans. All $^{15}$N NMR spectra were referenced to liquid $NH_3$ (20 °C), $\delta = 0$ ppm, by setting the isotropic ammonium $^{15}$N NMR peak of crystalline $^{15}NH_4{}^{15}NO_3$ to 23.8 ppm.[32,33]

Prior to analysis of MAS spectra, the spinning sidebands were summed to produce a pattern representative of the isotropic MAS NMR spectrum.[34] All spectra were analyzed using the WSolids software package, which was developed in this laboratory. WSolids incorporates the space-tiling algorithm of Alderman et al. for the efficient generation of powder spectra.[35] Best-fit spectra and uncertainties in parameters were determined by visual comparison of experimental and calculated spectra.

Ab initio chemical shielding calculations were carried out for **1**, **3, 4,** pyridine, and aniline, on an IBM RISC 6000 Work Station using *Gaussian 94*.[36] The molecular structures used in the calculations on the cobaloximes were taken from reported X-ray structures.[30,37,38] For pyridine and aniline, calculations were done on the ground-state MP2/6-311G* geometry-optimized structures, which are very close to experimentally determined geometries.[39,40] All chemical shielding calculations were performed using the gauge-independent atomic orbital (GIAO) method,[41] with both restricted Hartree−Fock (RHF) theory and density functional theory (DFT). Cobalt is a heavy fourth row element, and is subject to relativistic effects; thus, the cobalt atoms were treated with effective core potentials (ECPs), using the LANL2DZ basis set.[42] Due to the large size of the cobaloxime systems, locally dense basis sets were used.[43] In general, all atoms directly bonded to cobalt, as well as atoms in the axial moieties, were assigned large basis sets (6-31G** and 6-311G**). The remaining atoms were assigned the 3-21G basis set. DFT calculations were carried out using Becke's three-parameter hybrid[44] and the correlation functional of Lee, Yang, and Parr (B3LYP).[45] Absolute chemical shieldings, $\sigma$, were converted to the $^{15}$N chemical shift scale relative to the reference compound, $NH_3$ (*l*, 20 °C), by applying the formula $\delta = \sigma_{ref} - \sigma$, where $\sigma_{ref} = 244.6$ ppm.[46] The aniline N−H bond lengths in **4** were set to 0.998 Å, which is the N−H bond length determined from a microwave study of aniline.[39]

## Results and Discussion

**1. Nitrogen-15 CPMAS NMR Spectra of Cobaloximes.** Before presenting the results of this investigation, it is necessary to briefly outline the procedure used to analyze the $^{15}$N NMR spectra obtained with MAS. In particular, the influence of neighboring quadrupolar $^{59}$Co nuclei is considered. The effects of a quadrupolar nucleus, spin *S*, on the solid-state MAS NMR spectrum of a spin−spin coupled spin-1/2 nucleus are now well understood.[10−12,47−50] Qualitatively, the high-field approximation is not strictly valid for quadrupolar nuclei; thus, the eigenstates of the quadrupolar nuclei are not completely quantized in the direction of the magnetic field, and are described by linear combinations of the pure Zeeman states. In this regime, MAS does not average the direct dipolar interaction between the quadrupolar and spin-1/2 nuclei to zero. As a result, a distorted multiplet comprised of $2S + 1$ peaks is observed for the spin-1/2 nucleus.

First-order perturbation treatments have been developed to address this problem for cases in which the absolute value of $C_Q/(4S\ (2S - 1)) \ll \nu_S$. Here $C_Q$ is the nuclear quadrupolar coupling constant and $\nu_S$ is the Larmor frequency of the quadrupolar nucleus.[48,49,51] The transition frequencies of the spin-1/2 nucleus, $\nu_m$, are shifted by a residual dipolar coupling, *d*, such that

$$\nu_m = \nu_{iso} - mJ + \frac{S(S+1) - 3m^2}{S(2S-1)}\, d \qquad (1)$$

where *J* is the indirect spin−spin coupling constant, $m = S$, $S - 1$, ..., $-S$, and *d* is expressed as (in Hz)

$$d = \left(\frac{3C_Q R_{eff}}{20\nu_s}\right)[(3\cos^2\beta^D - 1) + \eta \sin^2\beta^D \cos 2\alpha^D] \qquad (2)$$

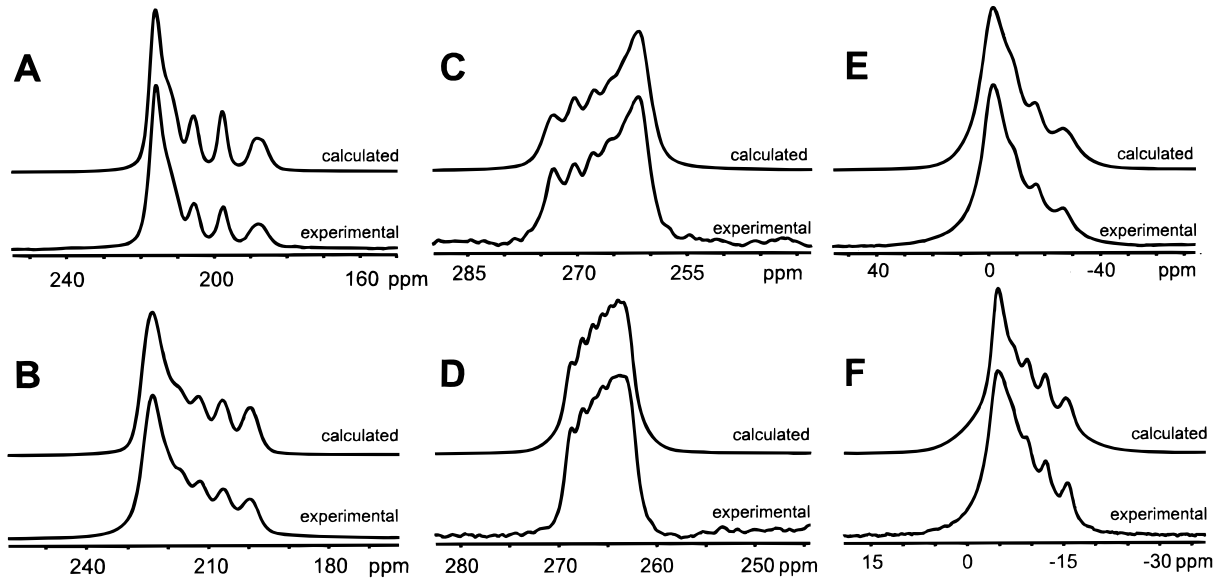


**Figure 2.** The isotropic peak in the experimental and calculated $^{15}$N CPMAS NMR spectra of $^{15}$N-enriched pyCo(DH)$_2$Cl (**1**) at (A) 4.7 T, $\nu_{rot}$ = 2729 Hz and (B) 9.4 T, $\nu_{rot}$ = 2557 Hz; of $^{15}$N-enriched pyCo(DH)$_2$CH$_3$ (**3**) at (C) 4.7 T, $\nu_{rot}$ = 3035 Hz and (D) 9.4 T, $\nu_{rot}$ = 3491 Hz; and of anilCo(DH)$_2$Cl (**4**) at (E) 4.7 T, $\nu_{rot}$ = 2251 Hz and (F) 9.4 T, $\nu_{rot}$ = 3371 Hz.

**TABLE 1: Parameters Obtained from Analysis of the $^{15}$N CPMAS NMR Spectra of $^{15}$N-Enriched Cobaloximes**

| compound | $\delta_{iso}$ (ppm) | $\lvert^1J(^{59}\text{Co}, ^{15}\text{N})\rvert$ (Hz)[a] | $R_{eff}$ (Hz)[b] | $C_Q$ (MHz)[c] | $\eta$[c] | $\beta^D$ | $\alpha^D$ | $d$ (Hz)[d] |
|---|---|---|---|---|---|---|---|---|
| $^{15}$N-pyCo(DH)$_2$Cl (**1**) | 207.9(2) | 74(2) | −378(20) | +64.82* | 0.63* | 0° | | 78 |
| $^{15}$N-pyCo(DH)$_2$Br (**2**) | 213.0(3) | 73(1) | −378(30) | +62(2) | n/a | 0° | | 74 |
| $^{15}$N-pyCo(DH)$_2$CH$_3$ (**3**) | 265.7(2) | 36(1) | −324(20) | +29.52* | 0.22* | 90° | 0° | −12 |
| $^{15}$N-anilCo(DH)$_2$Cl (**4**) | −7.9(1) | 63(3) | −353(20) | +80(3) | n/a | 0° | | 90 |

[a] The sign of $^1J(^{59}\text{Co},^{15}\text{N})$ cannot be determined from analysis of the MAS NMR spectra. [b] Effective dipolar coupling constant, $R_{eff} = R_{dd} - \Delta J/3$. [c] Parameters marked with an asterisk were reported in an NQR study by LaRossa and Brown.[8] [d] Calculated for $\nu_{Co-59}$ = 94.5 MHz ($B_0$ = 9.4 T).

If $d$ is positive, the "sense" of the spectrum is said to be positive, with the spacing between adjacent peaks increasing from high to low frequency. Conversely, if $d$ is negative, the spacing decreases from high to low frequency. In eq 2, $\alpha^D$ and $\beta^D$ are polar angles describing the orientation of the dipolar vector, $\mathbf{r}_{IS}$, with respect to the principal axis system (PAS) of the EFG tensor at the $S$ nucleus, and $\eta$ is the quadrupolar asymmetry parameter. The EFG tensor is traceless and is described by three principal components in its own principal axis system, defined such that $|V_{33}| \geq |V_{22}| \geq |V_{11}|$, with $C_Q = eQV_{33}/h$ and $\eta = (V_{11} - V_{22})/V_{33}$. $R_{eff}$ is the effective dipolar coupling constant, $R_{eff} = R_{dd} - \Delta J/3$, where the direct dipolar coupling constant, $R_{dd} = (\mu_0/4\pi)(\gamma_I\gamma_S\,\hbar/2\pi)\langle r_{IS}^{-3}\rangle$, and the anisotropy in the indirect spin−spin coupling is given by $\Delta J = J_{||} - J_\perp$ for an axially symmetric $J$-tensor.[52,53] Here, the motionally averaged inverse cube of the internuclear distance is designated by $\langle r_{IS}^{-3}\rangle$.

Recently, Olivieri and co-workers have emphasized that eqs 1 and 2 are dependent upon the relative signs of the magnetogyric ratios of the spin-1/2 and quadrupolar nuclei.[50,54] Equations 1 and 2 can be modified for cases when $\gamma_I$ is negative (as in the case of $\gamma_{N-15}$) by (i) removing the negative sign in front of "$mJ$" in eq 1, and (ii) placing a negative sign in front of the right-hand side of eq 2. This ensures that the transitions correspond to the proper spin states of the quadrupolar nucleus, and the same definitions for the "sense" of the multiplet are maintained. The signs of $J$ and $R_{eff}$ cannot be determined from the analysis of MAS NMR spectra using first-order perturbation theory; however, when first-order perturbation theory is not valid, observed spectra depend on the signs of these parameters.[50]

*A. Nitrogen-15 CPMAS NMR Spectra of $^{15}$N-Enriched pyCo(DH)$_2$Cl* (**1**). Experimental and calculated $^{15}$N CPMAS NMR spectra of **1** at both 4.7 and 9.4 T are shown in Figure 2A and 2B, respectively. The distorted multiplets result from the presence of residual dipolar coupling between $^{15}$N and $^{59}$Co. Since the degree of distortion is inversely dependent upon the $^{59}$Co Larmor frequency (see eq 2), the spectrum acquired at 4.7 T is more distorted than the corresponding spectrum at 9.4 T (i.e., five peaks are resolved at 9.4 T, as opposed to four at 4.7 T). The spacing between adjacent peaks increases from high to low frequency (left to right), meaning that the sense of the spectrum is positive. The parameters used to simulate these spectra are given in Table 1.

The analysis of the $^{15}$N CPMAS NMR spectra of **1** is aided by the availability of structural and nuclear quadrupole data obtained from various sources (vide infra). The $^{59}$Co, $^{15}$N direct dipolar coupling constant calculated from the Co, $N_{ax}$ internuclear distance, $r(\text{Co},N_{ax})$ = 1.965(3) Å,[37] is $R_{dd}$ = −378 Hz. Values of $C_Q$ = +64.82 MHz and $\eta$ = 0.63 are reported for **1**, from the $^{59}$Co NQR study of LaRossa and Brown.[8] The sign of $C_Q$ was predicted by a rough "donated charge" model, based on comparison of the relative partial field gradients of the axial and equatorial ligands. Using this same model, LaRossa and Brown also propose that the largest component of the EFG, $V_{33}$, is oriented along the L−Co−X axis. The $C_{2v}$ symmetry of the molecule dictates that if one of the EFG principal components is aligned in the direction of the axially bonded species, then the remaining components must lie in the plane of the DH moieties, with one component bisecting the dimethylglyoxime−cobalt ring, and the other bisecting the inter-ring N−Co−N bond

**TABLE 2: Comparison of $^1J(^{59}Co,^{15}N)$ and $^1J(^{103}Rh,^{15}N)$ in Cobaloximes and Rhodoximes ($LRh(DH)_2X$)**

| L, X | $^1J(^{59}Co,^{15}N)$ (Hz) | $^1K(Co,N)^a$ (N A$^{-2}$ m$^{-3}$) × $10^{21}$ | $^1J(^{103}Rh,^{15}N)$ (Hz) | $^1K(Rh,N)^b$ (N A$^{-2}$ m$^{-3}$) × $10^{21}$ | $^1K(Rh,N)/^1K(Co,N)$ |
|---|---|---|---|---|---|
| py, Me | −36 | 1.26 | 7.2 | 1.87 | 1.48 |
| py, Cl | −75 | 2.62 | 17.8 | 4.62 | 1.76 |

[a] Reduced indirect spin−spin coupling, $K(A,B) = (4\pi^2)\, J(A,B)/\gamma_A\gamma_B\, h$. [b] Data from ref 15.

angles.[55] This proposed orientation corresponds to $\beta^D = 0°$, for which $\alpha^D$ is undefined.

Several comments should be made about the NMR parameters extracted from our analysis. The magnitude of $^1J(^{59}Co,^{15}N)$, 74(2) Hz, is comparable to previously reported values of 62.5(1.0) Hz and 63.8(1.0) Hz in $[Co(NH_3)_5(^{15}NH_3)]^{3+}$ and tris-(ethylenediamine[$^{15}$N,$^{15}$N])-cobalt(III), respectively.[13] The spectrum can be simulated using the known EFG parameters, $\beta^D = 0°$, and $R_{eff} \simeq R_{dd}$; thus, anisotropy in the *J*-coupling is assumed to be small, i.e., $\Delta J \simeq 0$. This is a reasonable assumption, since $|\Delta J|$ is generally less than $|J|$, in cases where $\Delta J$ has been determined unambiguously.[56] If the same is true here, then the contribution from $\Delta J$ is minimal (i.e., $|\Delta J/3| < 25$ Hz) compared to the much larger value of $R_{dd}$. This assumption is in place for the remainder of the complexes examined in this paper. The polar angle $\beta^D$ indicates that the largest component of the EFG tensor, $V_{33}$, is oriented along the direction of the Co, $N_{ax}$ internuclear vector, in agreement with the proposed EFG tensor orientation of LaRossa and Brown.[8] In cases where $\beta^D = 0°$, $\eta$ has no effect on the appearance of the spectrum, since the last term of eq 2 is zero. The isotropic chemical shift of pyridine has been reported in the solid state as $\delta_{iso} = 299$ ppm[57] and 319 ppm.[18] The latter value is likely more reliable, since spectra were acquired using a modern NMR spectrometer at a higher applied field. The coordination of pyridine to the cobalt center in **1** results in a shielding of the nitrogen by approximately 111 ppm (coordination shift, $\Delta = \delta_{complex} - \delta_{free\ ligand} = -111$ ppm). Further comparison of the nitrogen magnetic shielding tensors of pyridine and **1** are made in section 2 of this paper.

*B. Nitrogen-15 CPMAS NMR Spectra of $^{15}$N-Enriched pyCo-(DH)$_2$Br* (**2**). In this case, neither the crystal structure nor quadrupolar parameters are available. However, a reasonable simulation of the $^{15}$N MAS NMR spectrum is possible provided that some prudent suppositions are made about the possible values of the unknown parameters. Slight structural changes have been observed in a comparison of the *trans*-influencing strengths of chlorine and iodine in $pyCo(DH)_2Cl$ and $pyCo(DH)_2I$.[58] Assuming that the bromine atom acts as a weak *trans*-influencing ligand, it is expected that despite its larger size, the overall effects on structure (e.g., $r(Co, N_{ax})$) will be similar to that of chlorine. Hence, $R_{dd}$ is assumed to be on the order of that for **1**. Comparison of the $^{15}$N CPMAS NMR spectra of **1** and **2** (not shown) reveal that these spectra are remarkably similar in appearance, with the only noticeable difference being the isotropic $^{15}$N chemical shift, with the $N_{ax}$ nucleus deshielded by 5 ppm in **2**. Calculations of these spectra yield parameters which are very similar (in fact, within experimental error) to those of **1**.

*C. Nitrogen-15 CPMAS NMR Spectra of $^{15}$N-Enriched pyCo-(DH)$_2$CH$_3$* (**3**). Replacement of weak *trans*-influencing anionic species such as halogens with strong $\sigma$-donors such as $CH_3^-$ is known[59] to have significant effects on the structure of cobaloximes, including a lengthening of the Co, L bond distance.[1,38] The analysis of the MAS NMR spectra of **3** is facilitated by the availability of both NQR and X-ray diffraction data. LaRossa and Brown report $C_Q = -29.52$ MHz and $\eta = 0.22$.[8] In addition, these authors suggest that the intermediate component of the EFG tensor, $V_{22}$, is aligned along the direction of the Co, $N_{ax}$ bond, which corresponds to $\beta^D = 90°$ and $\alpha^D = 90°$. The magnitudes of the quadrupolar parameters were confirmed by a recent solid-state $^{59}$Co NMR study by Frydman et al., who report $|C_Q| = 29.6(4)$ MHz and $\eta = 0.3(2)$.[6] Randaccio and co-workers[38] report $r(Co,N_{ax}) = 2.068(3)$ Å from which $R_{dd} = -324.4(5)$ Hz is calculated.

The $^{15}$N CPMAS NMR spectra of **3** (Figure 2C, 2D) are more symmetrical than those of **1** and **2**, with seven of the eight peaks of the multiplet resolved at 9.4 T. This is in accord with the smaller $C_Q$ observed in **3** relative to the former compounds. In addition, the sense of the spectrum is opposite to that for **1** and **2** (i.e., *d* is negative). The spacings between the peaks are reduced, and in contrast to the previous two cases, the indirect spin−spin coupling can be measured directly from the splitting between the two central peaks of the multiplet, as $|^1J(^{59}Co,^{15}N)| = 36(1)$ Hz. Using the proposed sign of $C_Q$ and the EFG tensor orientations of LaRossa and Brown, we found that it was impossible to properly simulate the MAS spectra; in fact, the entire sense of the spectrum is reversed (i.e., mirror images of the spectra pictured in Figure 2C,D). Our analyses reveal that the smallest component of the EFG tensor, $V_{11}$, is oriented along the Co, N internuclear vector, and that the sign of $C_Q$ is positive. Similar disagreement was found in a previous analysis of the $^{31}$P CPMAS NMR spectrum of $PPh_3Co(DH)_2CH_3$. In this case, $V_{11}$, as opposed to $V_{22}$, is oriented in the direction of the Co, P bond.[5] The substitution of the methyl anion into the axial position clearly has a marked effect on both the magnitude of the *J*-couplings, $C_Q$ and $\eta$, and the relative orientation of EFG and dipolar tensors.

There are not enough data available to make any definitive statements about the correlation between molecular structure and the magnitude of $^1J(^{59}Co,^{15}N)$, though in this work we observe an increase in $|^1J(^{59}Co,^{15}N)|$ with decreasing Co, N separation. Such relationships have been found in some cases for indirect spin−spin couplings between light and heavy nuclei, where the Fermi-contact mechanism[60] is thought to predominate.[61] However, there is increasing evidence that mechanisms other than the Fermi-contact mechanism are in general important and particularly, for example, if one member of the spin pair is a heavy nucleus, and the other is a second-row nucleus.[56,62]

A comparison of $^1J(^{59}Co,^{15}N)$ in **1** and **3** and $^1J(^{103}Rh,^{15}N)$ in the isostructural rhodoximes[15] is given in Table 2. As anticipated, the metal, nitrogen reduced spin−spin coupling constants increase with increasing atomic number, *Z*.[63,64]

Using the theory of Townes and Dailey,[65] the values of $C_Q(^{59}Co)$ in **1** and **2** relative to that in **3** can in part be attributed to the *s*-character involved in the Co, C and Co, $N_{ax}$ bonds. As the *s*-bonding character in a covalent bond increases, the EFG at the nucleus decreases, according to

$$eq_{zz} = (1 - s - i - \pi)eq_{at} \qquad (3)$$

where $eq_{zz}$ is the largest component of the EFG tensor, $eq_{at}$ is the atomic EFG (available from atomic data), and *s*, *i*, and $\pi$ are the *s*-, ionic, and $\pi$-bond characters. The decreased value

of $C_Q$ in **3** is consistent with the increased *s*-bonding character in the Co, C bond, which results from the presence of the strongly $\sigma$-donating axial methyl substituent. This methyl group is also believed to exhibit a strong electronic *trans*-influence, resulting in an increase in the Co, $N_{ax}$ bond length in **3**.[1,38] Due to reduced steric interactions between the pyridine and the planar DH moieties, it is expected that the cobalt atom will not be displaced from the plane to the same extent as in **1**, and that the DH nitrogen atoms should adopt an increasingly planar arrangement with respect to one another in **3**. Thus, the decrease in $C_Q$ in **3** can also be attributed to heightened symmetry about the Co atom.

*D. Nitrogen-15 CPMAS NMR Spectra of $^{15}$N-Enriched anilCo(DH)$_2$Cl* (**4**). From the X-ray structure of **4**,[30] the Co, $N_{ax}$ bond length is 2.010 Å, corresponding to $R_{dd} = -353$ Hz. Unlike compounds **1** and **3**, $C_Q(^{59}Co)$ and $\eta$ have not been measured for this complex. Thus, analysis of the MAS NMR spectra requires some well-founded assumptions in order to estimate the unknown quadrupolar parameters.

Comparison of the $^{15}$N CPMAS NMR spectra of **1** and **4** (Figure 2E,F) reveals that there are increased quadrupolar-induced distortions in the spectra of **4**, possibly indicating that $C_Q$ is larger in this complex (since $R_{dd}$ in **4** is smaller than in **1**). A large number of trial spectral simulations yielded the best fit parameters $|^1J(^{59}Co,^{15}N)| = 63(3)$ Hz and $\delta_{iso} = -7.9(1)$ ppm. Comparison with the isotropic chemical shift of neat liquid aniline, $\delta_{iso} = 58.2$ ppm,[66] demonstrates a similar coordination shift effect to that observed for the pyridine-substituted cobaloximes, with $\Delta = -66$ ppm (i.e., the coordinated aniline is more shielded than the free ligand). There are, however, several degenerate solutions which involve different values of $C_Q$ and distinct EFG orientations relative to the dipolar vector. The first and most reasonable solution has $C_Q = +80(3)$ MHz, with $V_{33}$ along the Co, N internuclear vector ($\beta^D = 0°$). If $\beta^D$ is set to 90°, there are a range of possible solutions involving changes in $\alpha^D$ and $\eta$. If $\alpha^D = 0°$ ($V_{11}$ along Co, N), the magnitude of $\eta$ has no effect on the appearance of the MAS spectrum; however, $C_Q = -160(4)$ MHz. Given the range of $C_Q$ reported by LaRossa and Brown for octahedral cobaloxime complexes (i.e., $|C_Q(^{59}Co)| = 28$ to 76 MHz), this solution is unlikely. When $\alpha^D = 90°$ ($V_{22}$ along Co, N), a variety of $C_Q$ and $\eta$ can be used for spectral calculations, ranging from $C_Q = -80$ MHz, $\eta \simeq 1$ to $C_Q = -160$ MHz, $\eta \simeq 0$. Decreasing the asymmetry parameter requires that the magnitude of $C_Q$ be increased well above the range of known $C_Q$ values (e.g., for $\eta = 0.7$, $C_Q \simeq 100$ MHz; $\eta = 0.5$, $C_Q \simeq 120$ MHz, etc.). Thus, from all the possible solutions, the most sensible is the first, with $\beta^D = 0°$ and $C_Q = +80(3)$ MHz.

A detailed comparison of the molecular structures of **1** and **4** may provide an explanation for the significantly larger $C_Q$ in **4**.[37,30] The increased EFG in **4** can in part be attributed to the *s*-character involved in the Co, N bond, according to the theory of Townes and Dailey (vide supra). In compound **1**, the pyridine nitrogen may crudely be regarded as an $sp^2$-hybridized nitrogen, while in **4**, the aniline nitrogen hybridization more closely resembles that of an $sp^3$ nitrogen. The decreased *s*-bonding character in **4** results in an increase in $eq_{zz}$, and therefore an increase in $C_Q$. In addition, the presence of the aniline group in **4** reduces the overall symmetry of the molecule to less than $C_{2v}$, since the aromatic ring of aniline is tilted over one of the DH moieties, with $\angle Co-N_{ax}-C = 120.7°$. This reduction in symmetry should lead to larger EFGs at the $^{59}$Co nucleus in **4**, also contributing to the increased $C_Q$ relative to that of **1**.

**2. Analysis of Nitrogen-15 NMR Spectra of Stationary Samples − Application of the Dipolar-Chemical Shift Method to $^{59}$Co, $^{15}$N Spin Pairs.** In its own principal axis system, the chemical shielding tensor is expressed in terms of three principal components which are defined from least to most shielded, $\sigma_{11} \leq \sigma_{22} \leq \sigma_{33}$ (or in terms of chemical shift, $\delta_{11} \geq \delta_{22} \geq \delta_{33}$). The orientation of the CS tensor in the molecular frame can be determined from single-crystal NMR studies.[67] However, in most instances single crystals suitable for such NMR studies are not available, and experiments must be conducted upon microcrystalline powder samples in which the molecules, and therefore the CS tensors, assume random distributions with respect to the applied magnetic field. Analysis of such spectra yield information on the principal components of the CS tensor, but not on the orientation of the CS tensor with respect to the frame of the molecule.

In situations where an isolated dipolar coupled spin pair is present, it is possible to gain information on the orientation of the CS tensor with respect to the internuclear dipolar vector, and therefore with respect to the molecular frame, using the dipolar chemical shift method.[17,68−72] At each of the discontinuities in the spectrum which correspond to the principal components of the CS tensor, there will be $2S + 1$ splittings which are dependent upon the magnitudes and relative sign of $R_{eff}$ and $J_{iso}$, as well as the orientation of the dipolar vector with respect to the chemical shielding tensor (given by the polar angles $\beta^C$ and $\alpha^C$). The approximate dipolar splittings, $\Delta\nu_{ii}$, at each principal component, $\delta_{ii}$, are given by

$$\Delta\nu_{11} = R_{eff}(1 - 3\cos^2\alpha^C \sin^2\beta^C)$$
$$\Delta\nu_{22} = R_{eff}(1 - 3\sin^2\alpha^C \sin^2\beta^C)$$
$$\Delta\nu_{33} = R_{eff}(1 - 3\cos^2\beta^C) \quad (4)$$

These expressions are strictly valid in cases where $\mathbf{r}_{IS}$ is aligned along any of the three principal components of the CS tensor.[72d,f] In addition, the overall splitting at each discontinuity will have a contribution from the isotropic *J*-coupling, observable only if it is of appreciable magnitude with respect to $\Delta\nu_{ii}$. As well, it has been demonstrated that relatively large quadrupolar interactions have minimal effects on the positions of the CS principal components or spectral extremities; however, some intensity redistribution over the powder pattern may occur.[72d,f,73] Thus, if $\mathbf{r}_{IS}$ is along the direction of one of the CS principal components, it is expected that eight ($2S + 1$) evenly spaced splittings should be observed at the discontinuities in the $^{15}$N NMR spectra of stationary samples.

*A. Nitrogen-15 NMR of Stationary Samples of $^{15}$N-Enriched pyCo(DH)$_2$Cl* (**1**). In this section, a detailed discussion of the interpretation of the stationary $^{15}$N NMR spectra of **1** is presented. The experimental and calculated $^{15}$N NMR spectra obtained at 9.4 T are pictured in Figure 3A. Analogous spectra were obtained at 4.7 T. The measurement of the dipolar splittings and the fitting of the spectra is abetted by the use of first-derivative NMR spectra (Figure 3B). It is useful to consider what information is already known about the NMR parameters and molecular structure of **1**. As discussed earlier, the effective dipolar coupling constant is approximated by $R_{dd}$, calculated from the known Co, N bond length, hence $R_{eff} = -378$ Hz. The magnitude of the indirect spin−spin coupling and the isotropic chemical shift have been measured from the MAS NMR spectra as $|^1J(^{59}Co,^{15}N)| = 74(2)$ Hz and $\delta_{iso} = 207.9(2)$ ppm. Thus, the unknown parameters are the span ($\Omega = \delta_{11} -$

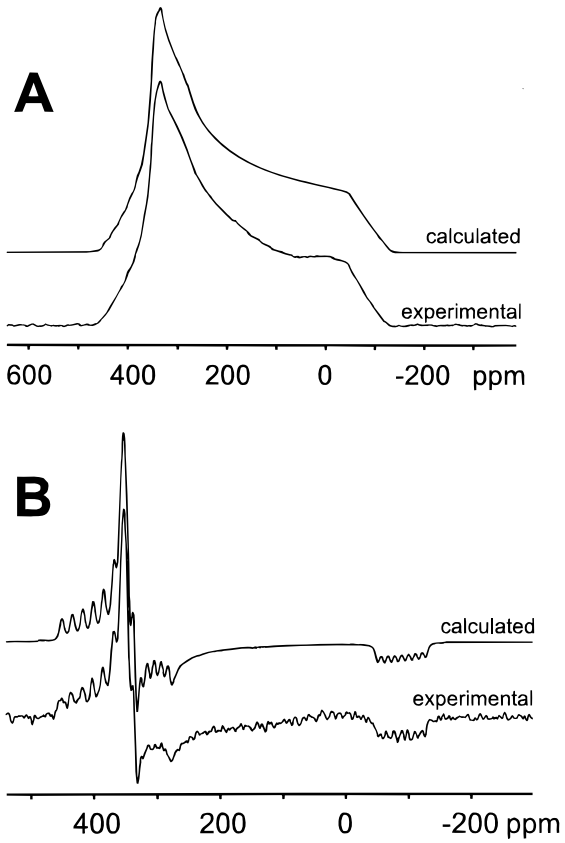


**Figure 3.** (A) Experimental and calculated $^{15}$N NMR spectra of stationary samples of $^{15}$N-enriched pyCo(DH)$_2$Cl at 9.4 T. (B) Corresponding first-derivative spectra.

$\delta_{33}$) and skew of the CS tensor ($\kappa = 3(\delta_{22} - \delta_{iso})/\Omega$),[74] and the polar angles $\beta^C$ and $\alpha^C$.

A suitable starting point for the analysis of these spectra is to measure the splittings at the discontinuity corresponding to $\delta_{33}$, which are ±441(15) Hz. No information is initially available on the signs of these splittings, but since the dipolar tensor is traceless, the sum of the measured $\Delta\nu_{ii}$ must be zero. Considering both positive and negative signs for $^1J(^{59}Co,^{15}N)$, it is determined that the best solution is $\Delta\nu_{33} = -367(15)$ Hz, $\beta^C = 84.3°$, which places $\delta_{33}$ approximately perpendicular to the dipolar vector. This orientation is in accordance with the high symmetry of the cobaloxime complex, and the perpendicular positioning of the pyridine ring with respect to the planar DH moieties, where it is expected that one of the CS tensor components at the pyridine nitrogen is oriented in the direction of the Co, N internuclear vector, with the remaining components perpendicular to the internuclear vector, oriented perpendicular to and in the plane of the pyridine ring.

With the new information on the apparent signs of $J$ and $\Delta\nu_{33}$, the angle $\alpha^C$ can be determined from the measurements of the splittings at $\delta_{11}$ or $\delta_{22}$. Measurements made at $\delta_{11}$ reveal a splitting of ±666(15) Hz. This corresponds to $\Delta\nu_{11} = +740$ Hz, from which $\alpha^C$ is calculated to be ca. 4°, corresponding to an orientation in which $\delta_{11}$ is aligned approximately in the direction of the Co, N bond.

Refinement of the parameters was achieved by calculating the $^{15}$N NMR spectra at both applied magnetic field strengths, with the final results presented in Table 3. The close agreement of the experimental and calculated spectra is especially apparent from close examination of the first-derivative spectra. Best-fit spectra were obtained with $^1J(^{59}Co,^{15}N) = -75(2)$ Hz. The powder pattern approaches axial symmetry as indicated by the skew, $\kappa = 0.70(2)$. The span observed at the pyridine nitrogen in **1**, $\Omega = 485(2)$ ppm, is notably reduced compared to that observed in the low-temperature solid-state NMR spectra of pyridine ($\Omega = 622(7)$ ppm).[18] Based on the CS tensor orientations from the solid-state $^{15}$N NMR study of pyridine,[57,18] it is likely that $\delta_{33}$ is oriented perpendicular to the pyridine ring plane. This is supported by the theoretical calculations presented in Section 3 of this paper.

*B. Nitrogen-15 NMR of Stationary Samples of $^{15}$N-Enriched pyCo(DH)$_2$Br* (**2**). The $^{15}$N NMR spectra of stationary samples of **2** were obtained at 4.7 and 9.4 T, and analyzed as described for **1** (spectra are not shown). The final parameters are presented in Table 3. The similarity of the NMR parameters of **1** and **2** obtained from spectra of stationary samples indicates that the substitution of bromine for chlorine into the axial position has very little effect on the molecular structure of the cobaloxime, in agreement with observations made earlier from the $^{15}$N MAS NMR spectra.

*C. Nitrogen-15 NMR of Stationary Samples of $^{15}$N-Enriched pyCo(DH)$_2$CH$_3$* (**3**). Analysis of $^{15}$N NMR spectra of stationary samples of **3** yielded the parameters given in Table 3. The span of the $^{15}$N CS tensor is similar to that observed in **1**, indicating that the presence of the axial methyl group does not influence the magnitude of the span significantly. However, the appearance of the spectra (not shown) indicates that the $^{15}$N CS tensor is very close to axial symmetry, with $\kappa = 0.96(4)$. The pyridine nitrogen nucleus in **3** is on average deshielded by ca. 58 ppm ($\delta_{iso} = 265.7(2)$ ppm) with respect to that in **1**. The intermediate component, $\delta_{22}$, is 103 ppm larger in **3**, whereas $\delta_{11}$ and $\delta_{33}$ are about 35 ppm larger. Despite the absence of resolved dipolar splittings, the spectra can only be simulated with $\beta^C$ set to 90°(4°), indicating that the orientation of the nitrogen CS tensor is similar to that in **1**. Varying $\alpha$ from 0° to 90° does not have any significant effects on the appearance of calculated spectra, since the magnitude of $\delta_{11}$ is very close to that of $\delta_{22}$. Changing the sign of $^1J(^{59}Co,^{15}N)$ from negative to positive does not have

**TABLE 3: Parameters Obtained from Dipolar-Chemical Shift Analysis of the $^{15}$N NMR Spectra of Stationary Samples of $^{15}$N-enriched Cobaloximes**

| compound | $\delta_{iso}$ (ppm)[a] | $\Omega$ (ppm) | $\kappa$ | $\delta_{11}$ (ppm) | $\delta_{22}$ (ppm) | $\delta_{33}$ (ppm) | $\beta^C$ | $\alpha^C$ | $R_{eff}$ (Hz) | $^1J(^{59}Co,^{15}N)$ (Hz) |
|---|---|---|---|---|---|---|---|---|---|---|
| $^{15}$N-pyCo(DH)$_2$Cl (**1**) | 207(1) | 484(2) | 0.70(2) | 393 | 320 | −92 | 85° | 3° | −375 | −75(2) |
| $^{15}$N-pyCo(DH)$_2$Br (**2**) | 212.5(2.0) | 485(7) | 0.72(2) | 396 | 328 | −89 | 88° | 2° | −372 | −73(2) |
| $^{15}$N-pyCo(DH)$_2$CH$_3$ (**3**) | 265(4) | 488(10) | 0.96(4) | 430 | 423 | −58 | 90° | *b* | −324 | −36(7) |
| $^{15}$N-anilCo(DH)$_2$Cl (**4**)[c] | | | | | | | | | | |
| Site 1 | −7.0(2.0) | 175(5) | 0.19(5) | 75 | 4 | −100 | 89(2)° | 3(1)° | −353 | −63(3) |
| Site 2 | −8.0(2.0) | 169(5) | 0.28(5) | 69 | 8 | −100 | 89(2)° | 6(1)° | −353 | −63(3) |

[a] $^{15}$N chemical shifts are referenced with respect to liquid $NH_3$ at 20 °C ($\delta_{iso} = 0.0$ ppm) by setting the chemical shift of the $^{15}$N ammonium resonance of $^{15}NH_4NO_3$ to 23.8 ppm. [b] $\alpha^C$ not determined, since $\delta_{11} \simeq \delta_{22}$. [c] Two magnetically nonequivalent sites with similar isotropic chemical shifts; $\delta_{33}$ can be determined precisely, but there is some overlap due to different values of $\delta_{11}$ and $\delta_{22}$ for each site, making exact determination of these parameters difficult.

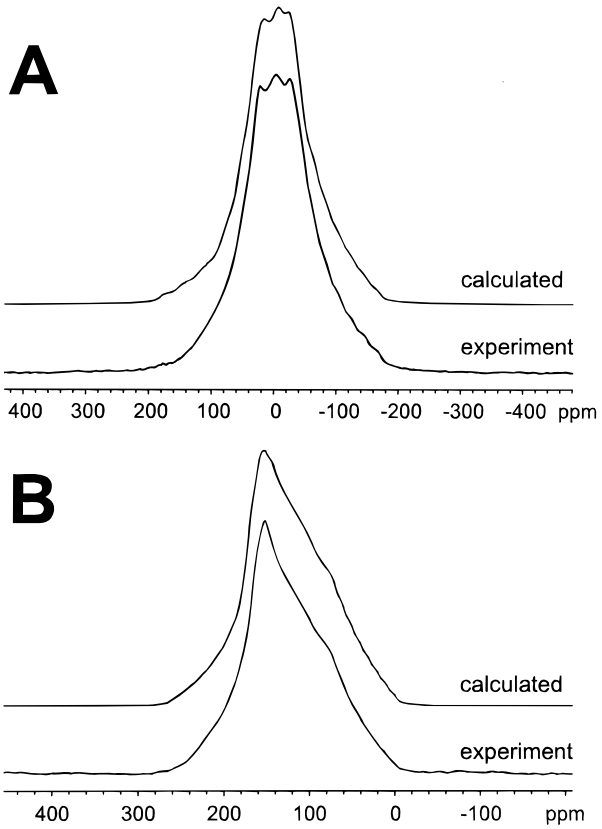


**Figure 4.** Experimental and calculated $^{15}$N NMR spectra of stationary samples of $^{15}$N-enriched anilCo(DH)$_2$Cl at (A) 4.7 T and (B) 9.4 T.

a noticeable effect on the spectral simulations, but given the sign of the previously determined *J*-couplings it is assumed that the sign of $^1J(^{59}\text{Co},^{15}\text{N})$ in **3** is negative.

*D. Nitrogen-15 NMR of Stationary Samples of $^{15}$N-Enriched anilCo(DH)$_2$Cl* (**4**). X-ray diffraction indicates that there are two crystallographically nonequivalent molecules in the unit cell of **4**.[30] Indeed, it was impossible to simulate the experimental spectrum shown in Figure 4 assuming one unique site. While the two nitrogen nuclei have very similar isotropic chemical shifts, there are differences in the principal components of the CS tensors. The values of $\delta_{33}$ are effectively identical, accounting for the well-defined splittings visible in the low-frequency region of the static spectrum. The high-frequency regions of the $^{15}$N powder patterns at both applied magnetic fields do not display well-defined splittings, due to an offset in the powder pattern of the two nonequivalent $^{15}$N nuclei in the regions corresponding to $\delta_{11}$ and $\delta_{22}$. This hampers the precise determination of $\delta_{11}$, $\delta_{22}$, and $\alpha^C$; nonetheless, clearly visible splittings in the $\delta_{33}$ regions of the spectra allow for determination of the nitrogen CS tensor orientations. Experimental information on the orientation of the nitrogen CS tensor in uncoordinated aniline is not currently available; therefore, assumptions about the orientation dependence of the chemical shielding cannot be made as easily as in the cases of **1**, **2**, and **3**. Ab initio calculations on aniline (vide infra) reveal that the span of the nitrogen CS tensor is ca. 80 ppm larger in the case of coordination of aniline to the cobalt atom.

The best-fit parameters defining the nitrogen CS tensor of the aniline nitrogen in **4** are given in Table 3. Spectral simulations incorporating a positive value of $^1J(^{59}\text{Co},^{15}\text{N})$ result in smaller splittings in the $\delta_{22}$ and $\delta_{33}$ regions; accordingly, the value of $^1J(^{59}\text{Co},^{15}\text{N})$ is negative as in the previous examples. The polar angles $\beta^C = 89°$ and $\alpha^C = 3°-6°$ reveal that $\delta_{11}$ is

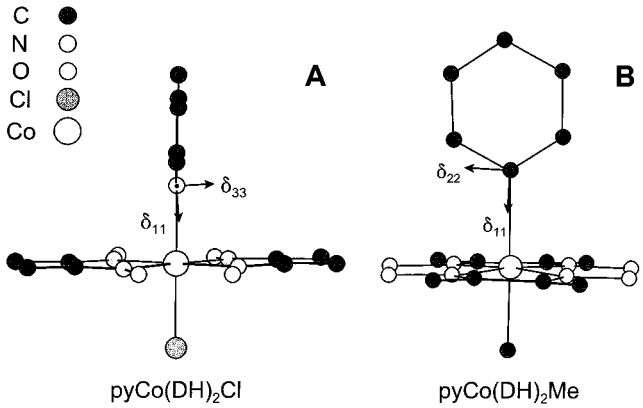


**Figure 5.** Nitrogen chemical shielding tensor orientations as determined by experimental methods and GIAO calculations in (A) $^{15}$N-pyCo(DH)$_2$-Cl, side view of the molecule, with the pyridine ring perpendicular to the page, and (B) $^{15}$N-pyCo(DH)$_2$CH$_3$, side view of the molecule, with the pyridine ring in the plane of the paper.

aligned approximately along the direction of the Co, N bond, with $\delta_{33}$ approximately perpendicular to the dipolar vector. It is likely that either $\delta_{22}$ or $\delta_{33}$ bisects the H−N−H bond angle. Ab initio calculations support this hypothesis, and are presented in the following section.

**3. Ab Initio Chemical Shielding Calculations.** In this section, comparison is made between experimental and calculated CS tensors in compounds **1**, **3**, and **4** (Table 4). The calculations correctly predict a negative coordination shift (i.e., increased nitrogen shielding upon coordination), and an increase in the span of the nitrogen CS tensor for uncoordinated pyridine with respect to that in **1** and **3**. Qualitative explanations are given which account for changes in the nitrogen CS tensors upon coordination to the cobalt atom.

The RHF calculations overestimate the span of the $^{15}$N CS tensor in **1** by over 100 ppm, with most of the contribution to the span arising from the $\delta_{33}$ component, which is predicted to be ca. 75 ppm less than the experimental value (note, a more negative chemical shift principal component indicates shielding at the nitrogen nucleus along the direction of that component; conversely, a positive shift in the principal component indicates deshielding along that direction). Moreover, the nitrogen nucleus is predicted to be shielded by 43 ppm (6-31G*) and 19 ppm (6-311G*). In the B3LYP/6-311G* calculations, the span is considerably closer to the experimental value, resulting from an overestimation of $\delta_{33}$, and a corresponding increase in $\delta_{iso}$ by ca. 70 ppm. The skews predicted by all of the calculations are in reasonable agreement with the experimental skew, confirming that the quasi-unique component is $\delta_{33}$. Given that these calculations are conducted on large, isolated molecules using a number of approximations (given in the Experimental Section), the qualitative agreement between theory and experiment is reasonable.

The most useful features of these calculations are the predicted CS tensor orientations in the molecular frame. In the RHF calculations with both basis sets, $\delta_{11}$ is oriented 0.7° from the Co, N bond, in good agreement with the experimentally determined orientations (see Figure 5A). The most shielded component, $\delta_{33}$, is found to lie perpendicular to the pyridine ring (88.2° with respect to the Co, N bond), in agreement with the experimentally determined CS tensor orientations in uncoordinated pyridine[18,57] and consistent with the experimental observation of $\beta^C = 85°$. This leaves $\delta_{22}$ oriented approximately in the ring plane (0.9° out of the plane). The B3LYP/6-311G*

**TABLE 4: Comparison of Experimental and Calculated Nitrogen Chemical Shielding Tensors[a]**

| | $\delta_{iso}$ (ppm) | $\Omega$ (ppm) | $\kappa$ | $\delta_{11}$(ppm) | $\delta_{22}$ (ppm) | $\delta_{33}$ (ppm) |
|---|---|---|---|---|---|---|
| py$Co(DH)_2Cl$ (**1**) | | | | | | |
| experimental | 207(1) | 484(2) | 0.70(2) | 393 | 320 | −92 |
| RHF/6-31G* | 164 | 595 | 0.43 | 419 | 249 | −177 |
| RHF/6-311G* | 188 | 623 | 0.44 | 453 | 279 | −170 |
| B3LYP/6-311G* | 273 | 506 | 0.9 | 454 | 416 | −52 |
| py$Co(DH)_2CH_3$ (**3**) | | | | | | |
| experimental | 265(4) | 488(10) | 0.97(8) | 430 | 423 | −58 |
| RHF/6-31G* | 230 | 542 | 0.72 | 437 | 360 | −105 |
| RHF/6-311G* | 257 | 570 | 0.73 | 472 | 396 | −98 |
| B3LYP/6-311G* | 291 | 533 | 0.75 | 491 | 423 | −42 |
| anil$Co(DH)_2Cl$ (**4**) | | | | | | |
| experimental | −7.0(3.0) | 175(3) | 0.18(2) | 75 | 4 | −100 |
| RHF/6-31G* | −59 | 224 | −0.34 | 65 | −84 | −159 |
| RHF/6-311G* | −51 | 230 | −0.33 | 77 | −77 | −154 |
| B3LYP/6-311G* | 40 | 73 | 0.58 | 70 | 54 | −3 |
| pyridine | | | | | | |
| experimental[b] | 299 | 782 | 0.44 | 633 | 414 | −149 |
| experimental[c] | 319 | 622 | 0.46 | 582 | 415 | −40 |
| RHF/6-31G* | 321 | 694 | 0.40 | 623 | 413 | −72 |
| RHF/6-311G* | 353 | 738 | 0.39 | 674 | 448 | −64 |
| B3LYP/6-31G* | 311 | 657 | 0.35 | 601 | 388 | −56 |
| B3LYP/6-311G* | 352 | 720 | 0.34 | 671 | 435 | −49 |
| LORG/[3s3p1d/2s][d] | 338 | 691 | 0.40 | 638 | 430 | −54 |
| IGLO/[5s4p1d/3s1p][e] | 349 | 721 | 0.43 | 658 | 451 | −63 |
| SOLO/[3s3p1d/2s][d] | 317 | 664 | 0.30 | 616 | 383 | −49 |
| aniline | | | | | | |
| experimental[f] | 58.2 | | | | | |
| RHF/6-31G* | 26 | 76 | 0.79 | 54 | 46 | −21 |
| RHF/6-311G* | 35 | 91 | 0.86 | 67 | 61 | −24 |
| B3LYP/6-31G* | 46 | 82 | 0.87 | 75 | 70 | −7 |
| B3LYP/6-311G* | 56 | 103 | 0.92 | 92 | 87 | −11 |

[a] Absolute chemical shieldings, $\sigma$, were converted to the $^{15}$N chemical shift scale relative to liquid $NH_3$ (20 °C) with the formula $\delta = \sigma_{ref} - \sigma$, where $\sigma_{ref} = 244.6$ ppm, the absolute chemical shielding of $NH_3$ at 20 °C.[46] [b] Data from ref 57. [c] Data from ref 18. [d] Data from ref 75. [e] Data from ref 77b. [f] Data from ref 66.

calculation, however, predicts that $\delta_{22}$ is 0.7° from the Co, N bond, and $\delta_{11}$ at 0.7° with respect to the pyridine ring, corresponding to polar angles of $\beta^C \simeq 90°$ and $\alpha^C \simeq 90°$, with $\delta_{33}$ still perpendicular to the pyridine ring plane. Spectral simulations were attempted with this relative tensor orientation without success, suggesting that the hybrid DFT method used here fails to correctly predict the nitrogen CS tensor orientations. This is not as serious as it might seem as the observed span of the nitrogen CS tensor is 484 ppm and $\delta_{11}$ and $\delta_{22}$ differ by only 73 ppm.

The best correspondence between theory and experiment is found for **3**. All calculations come close to predicting the span, skew, and isotropic shifts, with RHF and DFT calculations underestimating and overestimating $\delta_{33}$, respectively. RHF theory predicts that $\delta_{11}$ is along the Co, N bond, with $\delta_{33}$ perpendicular to the pyridine ring plane, and $\delta_{22}$ in the plane of the ring (Figure 5B), in excellent agreement with the experimental results. The calculations also correctly predict the overall deshielding of the nitrogen nucleus in **3** compared to **1**.

To qualitatively explain the nitrogen CS tensor orientations in **1** and **3**, it is worthwhile to consider the shielding in uncoordinated pyridine. Ab initio nitrogen CS tensors in pyridine are in very good agreement with the recently reported experimental values of Grant and co-workers.[18] There is also close agreement with the nitrogen CS tensors of pyridine calculated using IGLO and LORG methods (Table 4).[75] All of the calculations predict a larger span and deshielding of the uncoordinated pyridine nitrogen relative to nitrogen in **1** and **3**, in accordance with experimental observations. The predicted orientation of the nitrogen CS tensor in pyridine has $\delta_{33}$ perpendicular to the ring plane, and $\delta_{22}$ and $\delta_{11}$ in the plane with $\delta_{22}$ bisecting the ring (in the direction of the lone pair of electrons at nitrogen, Figure 6). Upon coordination, the least shielded component is now in the direction of the nitrogen lone pair, with $\delta_{22}$ perpendicular to the Co, N bond and in the ring plane. The orientation of $\delta_{33}$ remains perpendicular to the

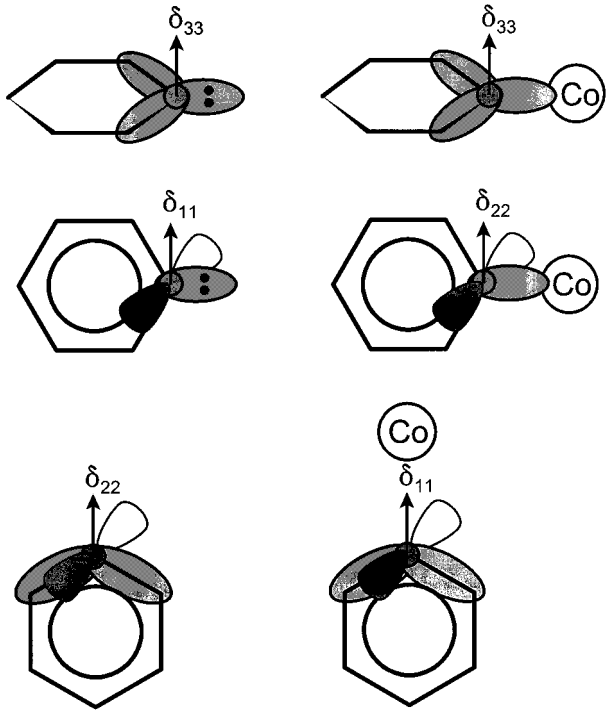


**Figure 6.** Nitrogen CS tensor components and associated molecular orbitals in pyridine and pyridine-substituted cobaloximes. See text for discussion.

pyridine ring, since there are no low-lying unoccupied states contributing to paramagnetic deshielding in this direction.

Grant and co-workers[18] have explained the nitrogen shielding tensor orientation in pyridine by considering contributions to chemical shielding from mixing of the ground- and excited-state molecular orbitals in Ramsey's equations for chemical shielding.[76] The paramagnetic contribution to shielding (i.e., normally deshielding) is inversely proportional to the energy difference between the ground- and appropriate excited-state orbitals; thus, the smaller the energy difference, the larger the deshielding at the nucleus. The principal components of the CS tensor are oriented perpendicular to the mixing molecular orbitals (vide infra), due to the nature of the angular momentum operators in Ramsey's equation.

In pyridine, the nitrogen nucleus is least shielded in the plane of the ring perpendicular to the nitrogen lone pair (Figure 6). This is due to paramagnetic deshielding dominated by contributions from low-energy $n \rightarrow \pi^*$ mixing (mixing orbitals are highlighted in the figure). Conversely, $\delta_{33}$ is oriented perpendicular to the ring plane, since there are no low-lying unoccupied states contributing to paramagnetic deshielding in this direction. Upon coordination to cobalt, the nitrogen lone pair occupies a high-energy bonding orbital with the cobalt nucleus. The absence of low-energy $n \rightarrow \pi^*$ mixing means that the nitrogen nucleus is generally more shielded in **1** (or **2**, **3**) than in pyridine. The nitrogen nucleus is deshielded along the direction of the Co, N bond. Here, $\delta_{11}$ is dominated by contributions from $\sigma_{N-C} \rightarrow \pi^*$ mixing. The $\delta_{22}$ component is oriented in the plane of the ring perpendicular to the Co, N bond, and is dominated by $\sigma_{N-Co} \rightarrow \pi^*$ mixing, which is slightly higher in energy than the corresponding $\sigma_{N-C} \rightarrow \pi^*$ mixing.

Calculations for **4** yield NMR parameters which are somewhat further from experimental results than those for **1** and **3**. RHF calculations overestimate the span by more than 55 ppm, and the DFT calculation underestimates the span by 102 ppm. In the former case, the calculated $\delta_{22}$ and $\delta_{33}$ components are much less than the experimental values, accounting for the larger span and increased nitrogen shielding. The DFT calculation suffers from an overestimation of $\delta_{11}$, resulting in the reduced span. None of the calculations predict the observed skew accurately.

RHF calculations once again predict a CS tensor orientation in good agreement with experimental data, with $\delta_{11}$ oriented 5.4° from the Co, N bond (Figure 7). The $\delta_{33}$ component is predicted to bisect the H−N−H bond angle of the aniline moiety, and lies perpendicular to the Co, N bond. The B3LYP calculation predicts that $\delta_{11}$ is oriented 20° from the Co, N bond, with the orientations of the remaining components having little correspondence to the local symmetry in the molecule. The agreement between RHF calculations and experimental results suggests that the former orientations are the most probable.

At this time, there is no experimental CS tensor information for aniline, though the nitrogen shielding tensor has been calculated using IGLO methods.[77] Our calculations reveal that $\delta_{11}$ is approximately perpendicular to the ring plane (Figure 8). All calculations predict that $\delta_{22}$ is 2.1° out of the aromatic plane at an angle ($\delta_{22}$−N−C) of 90°. Finally, $\delta_{33}$ bisects the H−N−H bond angle, and is oriented at an angle $\delta_{33}$−N−C = 175°. According to both RHF and DFT calculations, the nitrogen CS tensor of aniline changes only slightly upon coordination in a cobaloxime complex, with $\delta_{11}$ along the direction of the Co, N bond.

A qualitative explanation of the CS tensor orientations in aniline and in **4** is somewhat more complicated than for pyridine, **1** and **3**, since there is not an orthogonal arrangement of

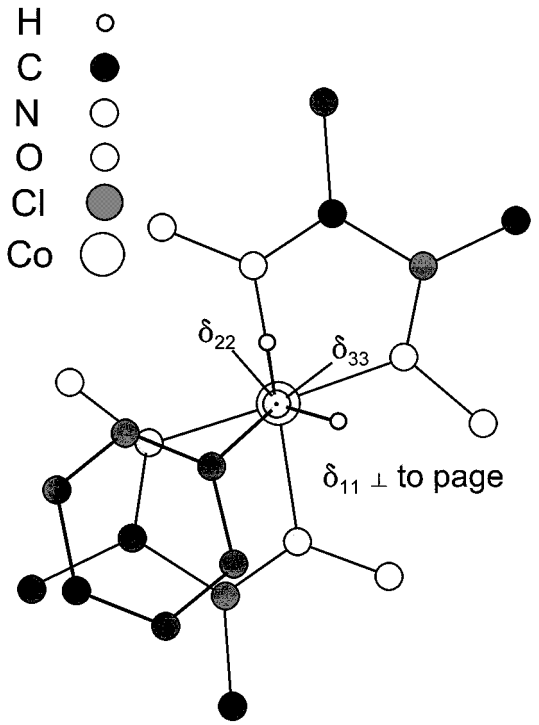


**Figure 7.** Nitrogen chemical shielding tensor orientation in $^{15}$N-anilCo(DH)$_2$Cl as determined by experimental methods and GIAO calculations. Top view of the molecule, with the dimethylglyoxime moieties in the plane of the page.

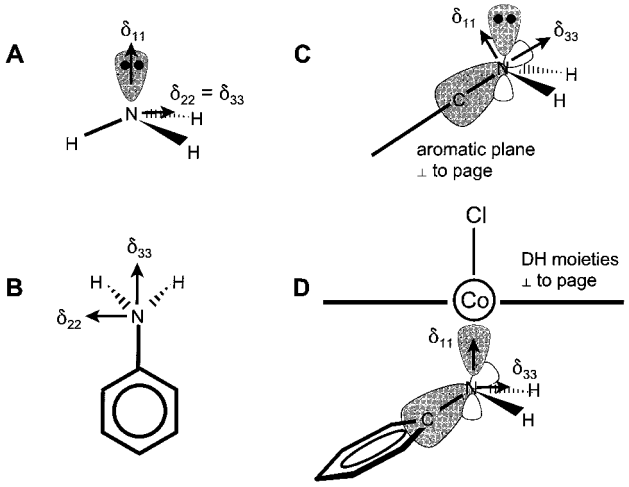


**Figure 8.** Nitrogen chemical shielding tensor orientations in (A) ammonia, (B), (C) aniline, and (D) aniline-substituted cobaloxime. See text for discussion.

molecular orbitals and CS tensor principal components. As a starting point, it is useful to consider ammonia (chemical shielding components: $\sigma_{11} = 237.7$ ppm and $\sigma_{22} = \sigma_{33} = 278.0$ ppm).[78] The least shielded component, $\sigma_{11}$, is along the direction of the lone pair, and is dominated by high-energy $\sigma \rightarrow \sigma^*$ mixing (Figure 8A). The low-energy $n \rightarrow \pi^*$ mixing, which results in large paramagnetic shielding contributions, is absent in ammonia, since the p-orbital character is very low. As a result, the nitrogen nucleus in ammonia is quite shielded. There is even less of a paramagnetic shielding contribution perpendicular to the lone pair, with $\sigma_{22}$ and $\sigma_{33}$ dominated by higher-energy $n \rightarrow \sigma^*$ mixing. In aniline, there is increased p-character at the nitrogen atom, since it is bound to an aromatic carbon (Figure 8B,C). As a result, the shielding at the nitrogen nucleus is governed by mixing of occupied states with virtual $\pi^*$ states,

hence, the nitrogen nucleus of aniline is deshielded compared to that of ammonia. The magnitudes of $\delta_{11}$ in aniline and **4** are very similar; however, in **4**, $\delta_{11}$ is oriented along the direction of the Co, N bond (Figure 8D). Magnetic shielding increases perpendicular to the Co, N bond, with reductions in both $\delta_{22}$ and $\delta_{33}$. This is due to the presence of high-energy $\sigma_{N-Co} \rightarrow \pi^*$ mixing, which accounts for the decreased isotropic shift in **4** relative to unbound aniline.

## Conclusions

The analysis of solid-state $^{15}$N NMR spectra of both spinning and stationary samples of the $^{15}$N-enriched cobaloximes has provided much information about the $^{59}$Co, $^{15}$N spin pair in these complexes. The magnitudes and signs of four previously unreported $^1J(^{59}Co,^{15}N)$ have been determined through combined analyses of $^{15}$N MAS NMR spectra influenced by residual dipolar coupling and $^{15}$N NMR spectra of stationary samples exhibiting splittings resulting from direct dipolar coupling to the $^{59}$Co nucleus. The magnitudes of the $^{59}$Co quadrupole coupling constants, asymmetry parameters, and the orientations of the $^{59}$Co EFG tensors are also reported. The orientations and chemical shift parameters of four $^{15}$N CS tensors have been determined, providing one of the first reports of CS tensor orientations for nitrogen nuclei directly bound to a transition metal center. The NMR parameters elicited from these spectra are very dependent upon the local and overall molecular geometry. The pyridine and aniline nitrogen nuclei experience greater shielding upon coordination to the cobalt center. Comparison of experimental CS tensors and those obtained via ab initio methods aids in confirming CS tensor orientations in the cobaloximes. There is a considerable amount of disparity between the experimental and theoretical CS principal components; nonetheless, the qualitative predictions made by the ab initio methods are in agreement with our experimental observations.

The acquisition of solid-state NMR spectra of a spin-1/2 nucleus coupled to a quadrupolar nucleus demonstrates that much information can be gained from such spectra that cannot be realized through analogous solution NMR experiments. It is hoped that this paper will encourage more work in determining NMR parameters from these solid-state methods, since they are capable of evoking detailed information on complex molecules.

**Acknowledgment.** We thank the Natural Sciences and Engineering Research Council (NSERC) of Canada for funding (REW) and the Atlantic Region Magnetic Resonance Centre (ARMRC) for the solid-state NMR facilities. R.W.S. thanks the Killam Trust and Walter C. Sumner Foundation for graduate fellowships. R.E.W. thanks the Canada Council for a Killam Research Fellowship. We are very grateful to Dr. Klaus Eichele for the development of the WSOLIDS software package, which is used extensively in our laboratory. Dr. Mike Lumsden and Ms. Myrlene Gee are thanked for acquiring some of the NMR spectra presented herein. We also thank Mr. Guy Bernard, Dr. Scott Kroeker, and Mr. David Bryce for their many helpful comments. Ms. Elinor Cameron is also given thanks for many crystal structure database searches.

## References and Notes

(1) Bresciani-Pahor, N.; Forcolin, M.; Marzilli, L. G.; Randaccio, L.; Summers, M. F.; Toscano, P. J. *Coord. Chem. Rev.* **1985**, *63*, 1.

(2) (a) Randaccio, L.; Bresciani-Pahor, N.; Zangrando, E.; Marzilli, L. G. *Chem. Soc. Rev.* **1989**, *18*, 225. (b) Finke, R. G.; Schiraldi, D. A.; Mayer, B. J. *Coord. Chem. Rev.* **1984**, *54*, 1. (c) Schrauzer, G. N.; Windgassen, R. J. *J. Am. Chem. Soc.* **1966**, *88*, 3738.

(3) (a) Hill, H. A. O.; Morallee, K. G. *J. Chem. Soc. (A)* **1969**, 554. (b) Trogler, W. C.; Stewart, R. C.; Epps, L. A.; Marzilli, L. G. *Inorg. Chem.* **1974**, *13*, 1564. (c) Gaus, P. L.; Crumbliss, A. L. *Inorg. Chem.* **1976**, *15*, 739. (d) Stewart, R. C.; Marzilli, L. G. *Inorg. Chem.* **1977**, *16*, 424. (e) Cartano, A. V.; Ingraham, L. L. *Bioinorg. Chem.* **1977**, *7*, 351. (f) Kargol, J. A.; Crecely, R. W.; Burmeister, J. L.; Toscano, P. J.; Marzilli, L. G. *Inorg. Chim. Acta* **1980**, *40*, 79. (g) Huet, J.; Gaudemer, A. *Org. Magn. Reson.* **1982**, *20*, 4. (h) Tavagnacco, C.; Balducci, G.; Costa, G.; Täschler, K.; von Philipsborn, W. *Helv. Chim. Acta* **1990**, *73*, 1469. (i) Brown, K. L.; Satyanarayana, S. *J. Am. Chem. Soc.* **1992**, *114*, 5674. (j) Moore, S. J.; Iwamoto, M.; Marzilli, L. G. *Inorg. Chem.* **1998**, *37*, 1169.

(4) Some recent solution NMR studies on cobalamins and cobalamides are (a) Brown, K. L.; Zou, X.; Webb, B. M. *Inorg. Chem.* **1994**, *33*, 4189. (b) Brown, K. L.; Zou, X. *Magn. Reson. Chem.* **1997**, *35*, 889. (c) Polson, S. M.; Cini, R.; Pifferi, C.; Marzilli, L. G. *Inorg. Chem.* **1997**, *36*, 314. (d) Kofod, P.; Harris, P.; Larsen, S. *Inorg. Chem.* **1997**, *36*, 2258. (e) Marzilli, L. G.; Polson, S. M.; Hansen, L.; Moore, S. J.; Marzilli, P. A. *Inorg. Chem.* **1997**, *36*, 3854.

(5) (a) Schurko, R. W.; Wasylishen, R. E.; Nelson, J. H. *J. Phys. Chem.* **1996**, *100*, 8057. (b) Schurko, R. W.; Wasylishen, R. E.; Moore, S. J.; Marzilli, L. G.; Nelson, J. H. *Can. J. Chem.* **1999**, *77*, 1973.

(6) Medek, A.; Frydman, V.; Frydman, L. *Proc. Natl. Acad. Sci. U.S.A.* **1997**, *94*, 14237.

(7) Asaro, F.; Gobetto, R.; Liguori, L.; Pellizer, G. *Chem. Phys. Lett.* **1999**, *300*, 414.

(8) LaRossa, R. A.; Brown, T. L. *J. Am. Chem. Soc.* **1974**, *96*, 2072.

(9) Power, W. P.; Kirby, C. W.; Taylor, N. J. *J. Am. Chem. Soc.* **1998**, *120*, 9428.

(10) Harris, R. K.; Olivieri, A. C. *Prog. NMR Spectrosc.* **1992**, *24*, 435.

(11) (a) Harris, R. K. In *Encyclopedia of Nuclear Magnetic Resonance*; Grant, D. M., Harris, R. K., Eds.; John Wiley & Sons: Chichester, U.K., 1996; pp 2909−2914. (b) McDowell, C. A. In *Encyclopedia of Nuclear Magnetic Resonance*; Grant, D. M., Harris, R. K., Eds.; John Wiley & Sons: Chichester, U.K., 1996; pp 2901−2908.

(12) Grondona, P.; Olivieri, A. C. *Concepts Magn. Reson.* **1993**, *5*, 319.

(13) Yamasaki, A.; Miyakoshi, Y.; Fujita, M.; Yoshikawa, Y.; Yamatara, H. *J. Inorg. Nucl. Chem.* **1979**, *41*, 473.

(14) (a) Bell, L. K.; Mingos, D. M. P.; Tew, D. G.; Larkworthy, L. F.; Sandell, B.; Povey, D. C.; Mason, J. *J. Chem. Soc. Chem. Commun.* **1983**, 125. (b) Bultitude, J.; Larkworthy, L. F.; Mason, J.; Povey, D. C.; Sandell, B. *Inorg. Chem.* **1984**, *23*, 3629.

(15) Rentsch, G. H.; Kozminski, W.; von Philipsborn, W.; Asaro, F.; Pellizer, G. *Magn. Reson. Chem.* **1997**, *35*, 904.

(16) Bose, K. S.; Abbott, E. H. *Inorg. Chem.* **1977**, *16*, 3190.

(17) Wasylishen, R. E.; Curtis, R. D.; Eichele, K.; Lumsden, M. D.; Penner, G. H.; Power, W. P.; Wu, G. In *Nuclear Magnetic Shieldings and Molecular Structure* − NATO ASI Series Vol. 386; Tossell, J. A., Ed.; Kluwer Academic Publishers: Dordrecht, The Netherlands, 1993; pp 297−314.

(18) Solum, M. S.; Altmann, K. L.; Strohmeier, M.; Berges, D. A.; Zhang, Y.; Facelli, J. C.; Pugmire, R. J.; Grant, D. M. *J. Am. Chem. Soc.* **1997**, *119*, 9804.

(19) Mason, J. In *Nuclear Magnetic Shieldings and Molecular Structure* − NATO ASI Series Vol. 386; Tossell, J. A., Ed.; Kluwer Academic Publishers: Dordrecht, The Netherlands, 1993; pp 449−471.

(20) Duncan, T. M. In *Principal Components of Chemical Shift Tensors: A Compilation*, − 2nd ed.; Farragut Press: Chicago, 1994.

(21) Mason, J.; Mingos, D. M. P.; Schaefer, J.; Sherman, D.; Stejskal, E. O. *J. Chem. Soc. Chem. Commun.* **1985**, 444.

(22) Santos, R. A.; Chien, W.-J.; Harbison, G. S.; McCurry, J. D.; Roberts, J. E. *J. Magn. Reson.* **1989**, *84*, 357.

(23) Groombridge, C. J.; Larkworthy, L. F.; Marécaux, A.; Povey, D. C.; Smith, G. W.; Mason, J. *J. Chem. Soc., Dalton Trans.* **1992**, 3125.

(24) Groombridge, C. J.; Larkworthy, L. F.; Mason, J. *Inorg. Chem.* **1993**, *32*, 379.

(25) Strohmeier, M.; Orendt, A. M.; Facelli, J. C.; Solum, M. S.; Pugmire, R. J.; Parry, R. W.; Grant, D. M. *J. Am. Chem. Soc.* **1997**, *119*, 7114.

(26) Salzmann, R.; Wojdelski, M.; McMahon, M.; Havlin, R. H.; Oldfield, E. *J. Am. Chem. Soc.* **1998**, *120*, 1349.

(27) Godbout, N.; Sanders, L. K.; Salzmann, R.; Havlin, R. H.; Wojdelski, M.; Oldfield, E. *J. Am. Chem. Soc.* **1999**, *121*, 3829.

(28) de Dios, A. C.; Roach, J. L. *J. Phys. Chem. A* **1999**, *103*, 3062.

(29) Trogler, W. C.; Stewart, R. C.; Epps, L. A.; Marzilli, L. G. *Inorg. Chem.* **1974**, *13*, 1564.

(30) Solans, X.; Font-Bardia, M.; López, C.; Alvarez, S. *Acta Crystallogr.* **1996**, *C52*, 63.
(31) Jameson, D. J.; Grzybowski, J. J.; Hammels, D. E.; Castellano, R. K.; Hoke, M. E.; Freed, K.; Basquill, S.; Mendel, A.; Shoemaker, W. J. *J. Chem. Educ.* **1998**, *75*, 447 and references therein.
(32) Hayashi, S.; Hayamizu, K. *Bull. Chem. Soc. Jpn.* **1991**, *64*, 688.
(33) Witanowski, M.; Stefaniak, L.; Webb, G. A. *Ann. Rep. NMR Spectrosc.* **1993**, *25*, 1.
(34) Wu, G.; Wasylishen, R. E. *J. Phys. Chem.* **1993**, *97*, 7863 and references therein.
(35) Alderman, D. W.; Solum, M. S.; Grant, D. M. *J. Chem. Phys.* **1986**, *84*, 3717.
(36) *Gaussian 94*, Revision B.2; Frisch, M. J.; Trucks, G. W.; Schlegel, H. B.; Gill, P. M. W.; Johnson, B. G.; Robb, M. A.; Cheeseman, J. R.; Keith, T.; Petersson, G. A.; Montgomery, J. A.; Raghavachari, K.; Al-Laham, M. A.; Zakrewski, V. G.; Ortiz, J. V.; Foresman, J. B.; Cioslowski, J.; Stefanov, B. B.; Nanayakkara, A.; Challacombe, M.; Peng, C. Y.; Ayala, P. Y.; Chen, W.; Wong, M. W.; Andres, J. L.; Replogle, E. S.; Gomperts, R.; Martin, R. L.; Fox, D. J.; Binkley, J. S.; Defrees, D. J.; Baker, J.; Stewart, J. P.; Head-Gordon, M.; Gonzalez, C.; Pople, J. A., Gaussian, Inc., Pittsburgh, PA, 1995.
(37) López, C.; Alvarez, S.; Aguilo, M.; Solans, X.; Font-Altaba, M. *Inorg. Chim. Acta* **1987**, *127*, 153.
(38) Bigotto, A.; Zangrando, E.; Randaccio, L. *J. Chem. Soc., Dalton Trans.* **1976**, 96.
(39) Lister, D. G.; Tyler, J. K. *J. Chem. Soc. Chem. Commun.* **1966**, 152.
(40) Bak, B.; Hansen-Nygaard, L.; Rastrup-Andersen, J. *J. Mol. Spectrosc.* **1958**, *2*, 361.
(41) (a) Wolinski, K.; Hinton, J. F.; Pulay, P. *J. Am. Chem. Soc.* **1990**, *112*, 8251. (b) Ditchfield, R. *Mol. Phys.* **1974**, *27*, 789.
(42) (a) Hay, P. J.; Wadt, W. R. *J. Chem. Phys.* **1985**, *82*, 270. (b) Wadt, W. R.; Hay, P. J. *J. Chem. Phys.* **1985**, *82*, 284. (c) Hay, P. J.; Wadt, W. R. *J. Chem. Phys.* **1985**, *82*, 299.
(43) (a) Chesnut, D. B.; Moore, K. D. *J. Comput. Chem.* **1989**, *10*, 648. (b) Chesnut, D. B.; Rusiloski, B. E.; Moore, K. D.; Egolf, D. A. *J. Comput. Chem.* **1993**, *14*, 1364.
(44) Becke, A. D. *J. Chem. Phys.* **1993**, *98*, 5648.
(45) Lee, C.; Yang, W.; Parr, R. G. *Phys. Rev. B* **1988**, *37*, 785.
(46) Jameson, C. J.; Jameson, A. K.; Oppusunggu, D.; Wille, S.; Burrell, P. M.; Mason, J. *J. Chem. Phys.* **1981**, *74*, 81.
(47) Menger, E. M.; Veeman, W. S. *J. Magn. Reson.* **1982**, *46*, 257.
(48) Olivieri, A. C.; Frydman, L.; Diaz, L. E. *J. Magn. Reson.* **1987**, *75*, 50.
(49) Apperly, D. C.; Haiping, B.; Harris, R. K. *Mol. Phys.* **1989**, *68*, 1277.
(50) Alarcón, S. H.; Olivieri, A. C.; Harris, R. K. *Solid State Nucl. Magn. Reson.*, **1993**, *2*, 325.
(51) Olivieri, A. C. *J. Magn. Reson.* **1989**, *81*, 201.
(52) Tutunjian, P.; Waugh, J. S. *J. Magn. Reson.* **1982**, *49*, 155.
(53) Wasylishen, R. E. *Encyclopedia of Nuclear Magnetic Resonance*; Grant, D. M., Harris, R. K., Eds.; John Wiley & Sons: Chichester, U.K., 1996; pp 1685−1695.
(54) Olivieri, A. C. *Magn. Reson. Chem.* **1996**, *34*, 365.
(55) Weil, J. A.; Buch, T.; Clapp, J. E. *Adv. Magn. Reson.* **1973**, *6*, 183.
(56) (a) Kroeker, S.; Hanna, J. V.; Wasylishen, R. E.; Ainscough, E. W.; Brodie, A. M. *J. Magn. Reson.* **1998**, *135*, 208 and references therein. (b) Bryce, D. L.; Wasylishen, R. E. *J. Am. Chem. Soc.*, in press.
(57) Schweitzer, D.; Speiss, H. W. *J. Magn. Reson.* **1974**, *15*, 529.
(58) Geremia, S.; Dreos, R.; Randaccio, L.; Tauzher, G. *Inorg. Chim. Acta* **1994**, *216*, 125.
(59) Appleton, T. G.; Clark, H. C.; Manzer, L. E. *Coord. Chem. Rev.* **1973**, *10*, 335.
(60) Ramsey, N. F. *Phys. Rev.* **1953**, *91*, 303.
(61) (a) Kunz, R. W. *Helv. Chim. Acta* **1980**, *63*, 2054. (b) Eichele, K.; Wasylishen, R. E. *Inorg. Chem.* **1994**, *33*, 2766.
(62) Lumsden, M. D.; Wasylishen, R. E.; Britten, J. F. *J. Phys. Chem.* **1995**, *99*, 16602 and references therein.
(63) Jameson, C. J. *Multinuclear NMR*; Mason, J., Ed.; Plenum Press: New York, 1987; pp 89−131.
(64) Dalling, D. K.; Gutowsky, H. S. *J. Chem. Phys.* **1971**, *55*, 4959.
(65) Dailey, B. P.; Townes, C. H. *J. Chem. Phys.* **1955**, *23*, 118.
(66) Lichter, R. L.; Roberts, J. D. *Org. Magn. Reson.* **1974**, *6*, 636.
(67) (a) Kennedy, M. A.; Ellis, P. D. *Concepts in Magn. Reson.* **1989**, *1*, 35. (b) Kennedy, M. A.; Ellis, P. D. *Concepts in Magn. Reson.* **1989**, *1*, 109.
(68) Oas, T. G.; Hartzell, C. J.; McMahon, T. J.; Drobny, G. P.; Dahlquist, F. W. *J. Am. Chem. Soc.* **1987**, *109*, 5956.
(69) Harris, R. K.; Packer, K. J.; Thayer, A. M. *J. Magn. Reson.* **1985**, *62*, 284.
(70) Zilm, K. W.; Grant, D. M. *J. Am. Chem. Soc.* **1981**, *103*, 2913.
(71) VanderHart, D. L.; Gutowsky, H. S. *J. Chem. Phys.* **1968**, *49*, 261.
(72) (a) Eichele, K.; Wasylishen, R. E. *J. Magn. Reson. A* **1994**, *106*, 46. (b) Power, W. P.; Wasylishen, R. E.; Curtis, R. D. *Can. J. Chem.* **1989**, *67*, 454. (c) Wasylishen, R. E.; Penner, G. H.; Power, W. P.; Curtis, R. D. *J. Am. Chem. Soc.* **1989**, *111*, 6082. (d) Eichele, K.; Lumsden, M. D.; Wasylishen, R. E. *J. Phys. Chem.* **1993**, *97*, 8909. (e) Wasylishen, R. E.; Wright, K. C.; Eichele, K.; Cameron, T. S. *Inorg. Chem.* **1994**, *33*, 407. (f) Wu, G.; Lumsden, M. D.; Ossenkamp, G. C.; Eichele, K.; Wasylishen, R. E. *J. Phys. Chem.* **1995**, *99*, 15806.
(73) (a) Casabella, P. A. *J. Chem. Phys.* **1964**, *41*, 3793. (b) VanderHart, D. L.; Gutowsky, H. S.; Farrar, T. C. *J. Am. Chem. Soc.* **1967**, *89*, 5056.
(74) Mason, J. *Solid State Nucl. Magn. Reson.* **1993**, *2*, 285.
(75) Bouman, T. D.; Hansen, A. E. *Chem. Phys. Lett.* **1992**, *197*, 59.
(76) Ramsey, N. F. *Phys. Rev.* **1950**, *78*, 699.
(77) (a) Schindler, M. *J. Am. Chem. Soc.* **1987**, *109*, 5950. (b) Schindler, M. *Magn. Reson. Chem.* **1988**, *26*, 394.
(78) Kukolich, S. G. *J. Am. Chem. Soc.* **1975**, *97*, 5704.